Tunneling emission from self-assembled InAs quantum dots probed with capacitance transients

Stephan Schulz, Andreas Schramm, Christian Heyn, and Wolfgang Hansen*
Institute for Applied Physics, University of Hamburg, Hamburg, Germany
(Received 25 January 2006; revised manuscript received 9 May 2006; published 27 July 2006)

The electron escape from self-assembled InAs quantum dots embedded in GaAs-Schottky diodes is probed with time-resolved capacitance measurements. We present the tunneling-transient spectroscopy technique to derive information on the barrier potential and the quantum dot level structure from the electric-field dependence of the capacitance transients. The data reveal that emission from *s*- and *p*-like quantum dot states can clearly be resolved. The barrier potential derived with this method in a simple triangular well model is in good agreement with values derived from measurements of the thermionic emission, if the emission from the *s*-type dot level is analyzed. The emission from dots occupied with more than one electron is discussed within a simple one-dimensional tunneling model. It reveals that the triangular well model underestimates the well potential by a value close to the Coulomb charging energy.

DOI: 10.1103/PhysRevB.74.033311 PACS number(s): 73.21.La, 73.23.Hk

Novel semiconductor-device concepts are based on the discrete charge-carrier states in self-assembled quantum dots (SAQDs). Thus not only for fundamental reasons, knowledge of the energy level structure as well as the carrier capture cross sections of SAQDs embedded in semiconductors is of crucial importance. Classical methods such as capacitance-voltage spectroscopy[1–4] as well as deep-level transient spectroscopy (DLTS)[5–10] are very powerful tools to obtain corresponding information. However, DLTS experiments on InAs SAQDs have been discussed with different models for the emission process.[7,10–13] It is suggested that the emission process involves tunneling from excited states so that the energies derived from conventional activation analysis does not reflect the barrier energy.[8,10,12] On the other hand, in Refs. 10 and 14 the activation energies determined from DLTS spectra are in agreement with values for energy level separations found by capacitance spectroscopy on samples with similar quantum dots. Furthermore, so far only simple single-particle models have been applied and the role of the Coulomb-addition energy remained unclear.[7,10–13,15] Moreover, in a recent work, Engström and Landsberg[16] point out that even without bringing tunneling processes into play, the presence of excited states leads to more complex emission paths than those assumed in the analysis of DLTS data published so far. The work establishes that dependent on the internal relaxation between ground and excited states in temperature-dependent measurements a transition region occurs, in which the dominant emission process changes. In a conventional Arrhenius analysis, this transition can be described by a temperature-dependent effective carrier capture cross section.[16] It is concluded that in the temperature range of the transition DLTS, results will be erroneous if a constant capture cross section is assumed.

In order to clarify the thermal emission path and the true barrier height for InAs SAQDs, it thus is very desirable to have an alternative method at hand in which emission from thermally occupied excited states is excluded. We apply a method that we call tunneling transient spectroscopy (TTS) in which the electron escape by pure tunneling processes is probed. Similar to DLTS, the electron occupation in the dots is measured via the capacitance across the depletion zone of the diode. The experiments are performed at such low temperature that thermal excitation does not play a role. The escape rates are probed as a function of the electric field applied at the quantum dots. Within models describing the electric field dependence of the tunneling rates, the binding energy of the dot states can be derived. Here by "binding energy" we mean the free energy necessary to remove an electron from the dot and add it to the continuum of the barrier material at the location of the dot.

The experiments are performed with Schottky diodes grown by molecular beam epitaxy on semi-insulating GaAs (100). They consist of slightly Si-doped ($N_D \approx 4\times10^{15}$ cm^{-3}) GaAs between a highly doped back contact (500 nm GaAs:Si, $N_D=2\times10^{18}$ cm^{-3}) and a metal gate (Cr, $\varnothing=1$ mm). A layer of InAs SAQDs is embedded in the low-doped GaAs layer. In the sample discussed in the following $N_D=3.7\times10^{15}$ cm^{-3} and the dot layer is located 755 nm below the surface of the diode. As indicated in the inset of Fig. 2, it is sandwiched between 10 and 5 nm thick undoped GaAs spacer layers. These are introduced in order to reduce the random potential in the dot layer due to ionized donors. For inspection with atomic force microscopy (AFM), the epitaxial growth of the sample is finished with a reference layer of InAs SAQDs grown at the same growth condition used for the embedded dot layer. From AFM inspection of the reference dot layer, we determine a dot density $N_{QD}=4.3\times10^{9}$ cm^{-2}.

During a filling voltage pulse applied between the contacts of the diode, the dots are loaded with electrons even at $T=10$ K. The capacitance transient of the diode is measured after the voltage has been reduced from the filling pulse value to the detection voltage V_r. At V_r, the dot layer is located within the depletion zone, the depth of which depending on the quantum-dot occupation. The transients thus reflect the time evolution of the dot occupation. Furthermore, the value of V_r determines the strength of the electric field at the quantum dot layer.

In Fig. 1, typical DLTS spectra of the diode are presented. They are recorded similarly to those published in earlier work.[10,14] We note that due to the presence of different emission paths and inhomogeneous broadening of the emission energies, the capacitance transients generally are not expo-

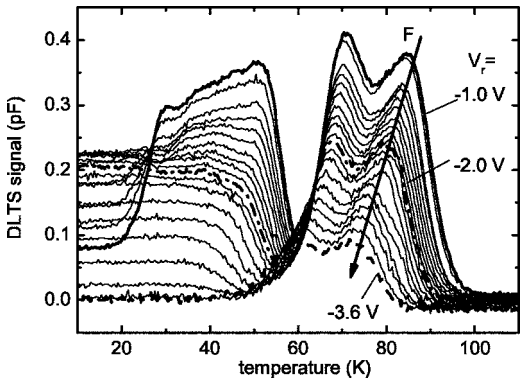

FIG. 1. DLTS spectra of a Schottky diode containing InAs quantum dots. Different spectra are recorded at different detection voltages V_r indicated. Highlighted by fat dashed, dashed dotted, and full lines are data recorded at the detection voltages indicated. The corresponding average electric fields are 1, 2, and 3.3×10^6 V/m, respectively.

nential and a rate window technique[17,18] must be employed to obtain the temperature-dependent DLTS signal. The DLTS spectra in Fig. 1 are determined from the capacitance transients using the double box car technique[10,17] with a reference time $\tau_{\mathrm{ref}}=4.04$ ms. The energies determined from the thermal emission of this sample are discussed in detail in Ref. 14. The conventional Arrhenius analysis of the trap signature assuming purely thermal activation from the localized dot states into the barrier continuum yields binding energies of 135 and 150 meV for emission from dots occupied with two and one electrons in the s state, respectively. These values are determined at a relatively low electric field of $F=1\times10^6$ V/m and found to strongly decrease with increasing electric field applied across the dots. A modified analysis basing on a thermionic tunneling model[10] yields slightly higher values: 151 and 165 meV for emission from doubly and singly occupied dots, respectively. Note that at temperatures below $T=20$ K, a temperature-independent DLTS signal occurs. A temperature-independent signal at low temperatures is generally associated to pure tunneling processes.[7] The signal is obviously strongly dependent on the detection voltage and thus on the average electric field in the dot layer.

In the following, this electric field dependence of the capacitance transients is studied in detail. In Fig. 2, a capacitance transient recorded at temperature $T=10$ K over a time of 4 days is depicted. The dot occupation is calculated from the capacitance difference to the value measured at the decharged dot layer. From the logarithmic scale it is obvious that the transient is not exponential at any time. This behavior persists even at times at which on average only less than one electron is contained in each dot. We attribute this to the inhomogeneous broadening of the dot energies and the effective electric field in the ensemble probed.

We thus employ a double box car filter in order to define a rate window. The difference $\Delta C=C(t_2)-C(t_1)$ of the capacitance values at two times t_1 and t_2 is depicted in Fig. 3 versus the electric field F. An effective electric field F at the quantum dot layer is calculated from the detection bias V_r and the measured capacitance assuming that charges in the

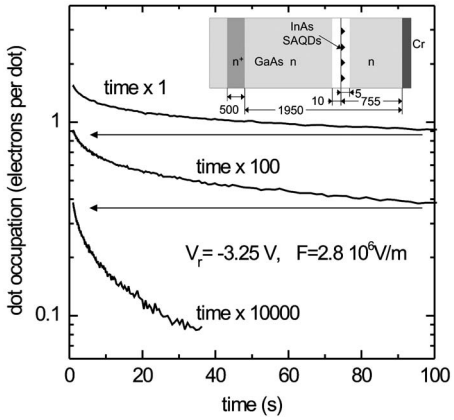

FIG. 2. Dot occupation calculated from a capacitance transient of a Schottky diode with SAQDs. The detection voltage was set to $V_r=-3.25$ V. This corresponds to an average electric field of $F=2.8\times10^6$ V/m. The time scale has to be multiplied by 100 and 10^4 for the middle and bottom trace, respectively. The inset depicts the layer structure of the Schottky diode. The numbers denote the layer thicknesses in nm.

dots do not contribute. In the following, we will first discuss the data with a model describing the dependence of the tunneling rate on this field. The additional Coulomb field of the dot charges is considered afterwards in the discussion of Fig. 4.

If the signal results from purely exponential decays, it will be dominated by those with rate close to $1/\tau_{\mathrm{ref}}=\ln(t_2/t_1)/(t_2-t_1)$. At the maxima, the reference time is thus associated with the tunneling time τ of the corresponding emission process. In the data of Fig. 3, clearly two maxima are resolved. Since tunneling rates are expected to increase with the electric field, we associate the maximum at lower

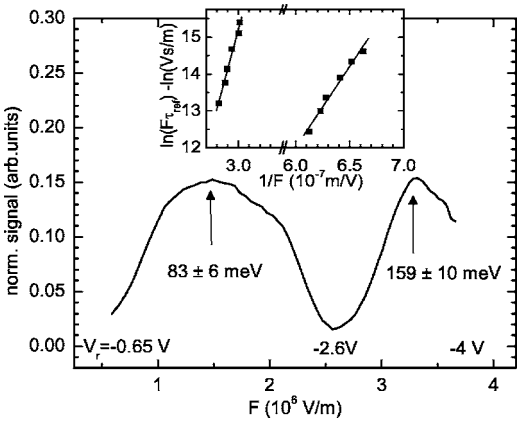

FIG. 3. TTS spectrum showing the capacitance change associated to tunnel emission from the quantum dots measured at a reference time $\tau_{\mathrm{ref}}=1467$ ms using $t_2/t_1=2$ and temperature $T=10$ K. The capacitance signal is normalized accounting for the dependence of the signal on the detection voltage. The detection voltages V_r used at the beginning, the minimum, and the end of the trace are denoted. The inset presents the logarithms of the reference times vs the inverse fields at the peak positions. Note that the x scale is broken. From the slope of the linear fits (full lines), the energies allocated to the peak positions are determined.

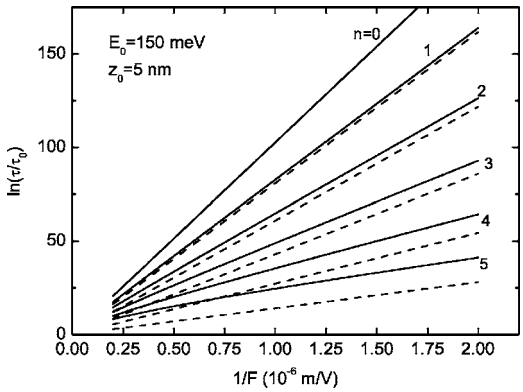

FIG. 4. The electric-field dependence of the tunneling time calculated with a one-dimensional WKB model (full traces). The field is the average electric field at the quantum-dot layer, which is controlled with the voltage applied at the diode. The numbers n at different traces reflect the dot occupation after emission of one electron. A dot radius $z_0=5$ nm is assumed giving a single electron addition energy $E_c=20$ meV. Dashed traces are calculated with Eq. (1) assuming the energies $E_{0,n}$ are lifted by the classical Coulomb charging energy as described in the text.

field to emission through shallower barriers. In correspondence with previous DLTS data, we associate the maxima to emission from the s and p levels.

In the following we use simple models to describe the electric-field dependence of the tunneling rates. The escape rate from a Dirac well potential through a triangular barrier is[19]

$$\tau^{-1} = \frac{eF}{4\sqrt{2m^* E_i}} \exp\left(-\frac{4}{3}\frac{\sqrt{2m^*}E_i^{3/2}}{e\hbar F}\right), \tag{1}$$

where F is the electric field describing the barrier slope and E_i is the binding energy. The effective mass is assumed to be the conduction-band edge mass of GaAs: $m^\star=0.067m_e$, where m_e is the free-electron mass. The inset of Fig. 3 shows how the field position of the peaks associated to tunneling from the s- and p-level shift in spectra taken at different τ_{ref}. In spectra recorded at rate windows with larger (smaller) reference time, the peaks occur at lower (higher) electric fields. According to Eq. (1), the data points should lie on a straight line with a slope from which the binding energy E_i can be determined. The numbers at the peaks in Fig. 3 are determined in this way. The error intervals quoted at the energies indicate the variation of the results that we obtain if we take the additional field of up to six electrons per dot homogeneously distributed in the dot layer into account. We note that the value of 159 meV is in very good agreement with the value for the s-level binding energy previously determined from DLTS experiments.[10,14] Also, the p-state binding energy of 83 meV is close to the activation energies determined for the p-level peaks. We note, however, that the triangular potential model may be expected to yield poor results since the repulsive Coulomb potential of the electrons occupying the dots adds to the barrier potential.

The Coulomb repulsion of charged dots can be considered within a simple one-dimensional model in which the triangular barrier potential is replaced by

$$V_B(z) = E_i - eFz - \frac{ne^2}{4\pi\varepsilon\varepsilon_0}\left[\frac{1}{z_0} - \frac{1}{z_0+z}\right], \tag{2}$$

where $z>0$ points against growth direction and z_0 is an approximate value for the dot radius. Since the electrons will favor the shortest tunneling path, the one-dimensional model may be good despite its simplicity. The electron interaction is approximated by the simplest classical model, in which the dot charged with n electrons is represented by a metallic sphere of radius z_0.

We approximate the exponential factor, which rules the tunneling rate, using a WKB ansatz with the barrier potential given by Eq. (2),

$$\tau^{-1} = \frac{1}{\tau_0(F)} \exp\left(-\frac{\sqrt{2m^*}}{\hbar}\int_0^{z_1}\sqrt{V_B(z)}dz\right), \tag{3}$$

where z_1 is the distance at which the barrier potential reaches the value of the energy level from which tunneling takes place. The preexponential factor is assumed to be moderately field-dependent as in case of the Dirac well [Eq. (1)], where it is linear. Numerical values for the exponential factor are depicted as full lines in Fig. 4. Similar to the triangular barrier model, the data form straight lines in good approximation at the experimental fields. The dashed lines in Fig. 4 are calculated with Eq. (1) replacing the binding energy E_i by $E_{i,n}=E_i-nE_c$ with the addition energy $E_c=e^2/(4\pi\varepsilon\varepsilon_0 z_0)$. Note that even in dots occupied with five electrons, both models predict the same slope. From this result we conclude that the analysis of the experimental data based on the triangular barrier model yields the binding energies reduced by the addition energies at dot occupations and fields of our experiments.

The electric field of the charges in the dots can be divided in a short-range and a long-range contribution. At the electric fields applied in the experiment, the field dependence of the tunneling rate is determined by the long-range contribution that is well approximated by a linear term which slightly increases the slope of the triangular barrier potential. The short-range term in essence leads to a lifting of the dot levels with respect to the interaction free barrier potential by an amount close to the Coulomb addition energy. If the resolution of the experiment suffices, the dot occupation dependent tunneling rates should result in a splitting of the s and p peaks into two and four maxima, respectively. However, at present the resolution seems to be too low to prove substructure unequivocally. We attribute the slightly lower resolution as compared to the DLTS spectra to the fact that the TTS spectra are more sensitive to field inhomogeneity. More investigations on samples of different doping and dot densities are in progress.

In order to compare the energies associated in Fig. 3 to the s and p peak with the single-particle level energies determined in previous DLTS and capacitance measurements on similar InAs SAQDs, we assume that at the p maximum the dots are on average occupied with three additional electrons as compared to the state from which electrons tunnel at

the *s* maximum. The single-particle *s*-*p* level spacing thus is given by the difference of the energies quoted in Fig. 3 reduced by the Coulomb addition energy that is necessary to increase the dot occupation from 1 to 4. If we adopt the harmonic-oscillator confinement model,[20] the interaction contributions to the level energies add to 7/4 times the Coulomb addition energy $E_c \approx 20$ meV of the second electron in the *s* shell. With this value we get an *s*-*p* level spacing of 41 meV, which is very close to values found previously.

In conclusion, the TTS method gives us an alternative to the DLTS method in cases where a complex scenario involving different emission paths may rule the thermal emission, so that the analysis of DLTS data becomes very involved. Here we study InAs quantum dots, in which excited states may lead to a multitude of emission paths. In the TTS method we probe the electric-field dependence of tunneling rates and compare results to a triangular barrier model. The barrier energies that best describe the data assigned to the tunnel escape from the *s*-type level are very close to those found from measurements of thermionic escape. From this we conclude that in the temperature range probed in our DLTS experiments on InAs SAQDs, one emission path dominates. Furthermore, in the TTS spectra a second maximum is clearly resolved that we associate with emission from *p* states. The triangular barrier model is extended in order to take into account the electron occupation of the dots. The field dependence of the tunneling rates calculated within a one-dimensional WKB model is similar to the triangular model at the experimental dot occupations and electric fields. The results show that at low occupation, the barrier energies can still be derived with the triangular barrier model provided the Coulomb charging energy is taken into account.

We gratefully acknowledge help from T. Zander and J. Schaefer. This work was funded by the Deutsche Forschungsgemeinschaft via SFB508 "Quantum Materials."

*Electronic address: hansen@physnet.uni-hamburg.de

[1] H. Drexler, D. Leonard, W. Hansen, J. P. Kotthaus, and P. M. Petroff, Phys. Rev. Lett. **73**, 2252 (1994).
[2] B. T. Miller, W. Hansen, S. Manus, R. J. Luyken, A. Lorke, J. P. Kotthaus, S. Huant, G. Medeiros-Ribeiro, and P. M. Petroff, Phys. Rev. B **56**, 6764 (1997).
[3] R. Wetzler, A. Wacker, E. Scholl, C. M. A. Kapteyn, R. Heitz, and D. Bimberg, Appl. Phys. Lett. **77**, 1671 (2000).
[4] K. H. Schmidt, C. Bock, M. Versen, U. Kunze, D. Reuter, and A. D. Wieck, J. Appl. Phys. **95**, 5715 (2004).
[5] S. Anand, N. Carlsson, M.-E. Pistol, L. Samuelson, and W. Seifert, Appl. Phys. Lett. **67**, 3016 (1995).
[6] S. Anand, N. Carlsson, M.-E. Pistol, L. Samuelson, and W. Seifert, J. Appl. Phys. **84**, 3747 (1998).
[7] C. M. A. Kapteyn, F. Heinrichsdorff, O. Stier, R. Heitz, M. Grundmann, N. D. Zakharov, D. Bimberg, and P. Werner, Phys. Rev. B **60**, 14265 (1999).
[8] C. M. A. Kapteyn, M. Lion, R. Heitz, D. Bimberg, P. Brunkov, B. V. Volovik, S. G. Konnikov, A. R. Kovsh, and V. M. Ustinov, Appl. Phys. Lett. **76**, 1573 (2000).
[9] O. Engström, M. Malmkvist, Y. Fu, H. O. Olafson, and E. O. Sveinbjörnsson, Appl. Phys. Lett. **83**, 3578 (2003).
[10] S. Schulz, S. Schnüll, C. Heyn, and W. Hansen, Phys. Rev. B **69**, 195317 (2004).
[11] S. K. Zhang, H. J. Zhu, F. Lu, Z. M. Jiang, and X. Wang, Phys. Rev. Lett. **80**, 3340 (1998).
[12] W.-H. Chang, W. Y. Chen, M. C. Cheng, C. Y. Lai, T. M. Hsu, N.-T. Yeh, and J.-I. Chyi, Phys. Rev. B **64**, 125315 (2001).
[13] O. Engström, M. Kaniewska, Y. Fu, J. Piscator, and M. Malmkvist, Appl. Phys. Lett. **85**, 2908 (2004).
[14] S. Schulz, A. Schramm, T. Zander, C. Heyn, and W. Hansen, in *Proceedings of the 27th International Conference on the Physics of Semiconductors, Flagstaff, Arizona, 2005*, edited by J. Menendez and C. G. V. de Walle, AIP Conf. Proc. No. 772 (AIP, New York, 2005), p. 807.
[15] W.-H. Chang, W. Y. Chen, T. M. Hsu, N.-T. Yeh, and J.-I. Chyi, Phys. Rev. B **66**, 195337 (2002).
[16] O. Engström and P. T. Landsberg, Phys. Rev. B **72**, 075360 (2005).
[17] D. V. Lang, J. Appl. Phys. **45**, 3023 (1974).
[18] P. Blood and J. Orton, *The Electrical Characterization of Semiconductors: Majority Carriers and Electron States*, edited by N. H. March (Academic Press, London, 1992).
[19] E. N. Korol, Sov. Phys. Solid State **8**, 1327 (1977).
[20] R. J. Warburton, B. T. Miller, C. S. Dürr, C. Bödefeld, K. Karrai, J. P. Kotthaus, G. Medeiros-Ribeiro, P. M. Petroff, and S. Huant, Phys. Rev. B **58**, 16221 (1998).